Journal of Forestry Research (2024) 35:20
https://doi.org/10.1007/s11676-023-01664-9

ORIGINAL PAPER

Dendroclimatological study of *Sabina saltuaria* and *Abies faxoniana* in the mixed forests of the Qionglai Mountains, eastern Tibetan Plateau

Teng Li[1] · Jianfeng Peng[2] · Tsun Fung Au[3,4] · Jingru Li[2] · Jinbao Li[5,6] · Yue Zhang[1]

Received: 19 June 2023 / Accepted: 5 July 2023

Abstract Tree-ring chronologies were developed for *Sabina saltuaria* and *Abies faxoniana* in mixed forests in the Qionglai Mountains of the eastern Tibetan Plateau. Climate-growth relationship analysis indicated that the two co-existing species reponded similarly to climate factors, although *S. saltuaria* was more sensitive than *A. faxoniana.* The strongest correlation was between *S. saltuaria* chronology and regional mean temperatures from June to November. Based on this relationship, a regional mean temperature from June to November for the period 1605–2016 was constructed. Reconstruction explained 37.3% of the temperature variance during th period 1961–2016. Six major warm periods and five major cold periods were identified. Spectral analysis detected significant interannual and multi-decadal cycles. Reconstruction also revealed the influence of the Atlantic Multi-decadal Oscillation, confirming its importance on climate change on the eastern Tibetan Plateau.

Keywords Tree-ring analysis · Mixed forests · Dendroclimatology · Qionglai Mountains

Introduction

The Tibetan Plateau has long been considered as the roof of the world, and is the largest plateau in China and the world's highest. The Plateau affects climate at regional and global scales and receives considerable attention in the study of large-scale climate change (Liu and Zhang 1998; Liu and Chen 2000; Liu et al. 2009; Yang 2012). The Plateau is one of the more sensitive and vulnerable regions in terms of climate change (IPCC 2013; Zhu et al. 2016; Li and Li 2017). However, scarce instrumental records make it difficult to fully understand the effects of climate change on the Plateau. Proxy records are essential to studies of long-term climate change on the Plateau. Among them, tree-rings have been widely used owing to the annual resolution, accurate dating,

Project funding: This study was supported by the National Key Research and Development Program of China (No. 2018YFA0605601), Hong Kong Research Grants Council (No. 106220169), and the National Natural Science Foundation of China (Nos. 41671042, 42077417, 42105155, and 42201083), and the National Geographic Society (No. EC-95776R-22).

Corresponding editor: Tao Xu.

✉ Yue Zhang
zhangyue@gzhu.edu.cn

Teng Li
liteng@gzhu.edu.cn

[1] School of Geography and Remote Sensing, Guangzhou University, Guangzhou 510006, People's Republic of China

[2] College of Geography and Environmental Science, Henan University, Kaifeng 475004, People's Republic of China

[3] Institute for Global Change Biology, School for Environment and Sustainability, University of Michigan, Ann Arbor, MI, USA

[4] Department of Ecology and Evolutionary Biology, University of Michigan, Ann Arbor, MI, USA

[5] Department of Geography, University of Hong Kong, Hong Kong SAR, People's Republic of China

[6] HKU Shenzhen Institute of Research and Innovation, Shenzhen 518057, People's Republic of China

Published online: 09 December 2023

and high sensitivity to climate in many regions around the globe (Fritts 1976; Schweingruber 1996; Shao 1997; Gou et al. 2010; Peng et al. 2014). Numerous dendroclimatological studies have been carried out on the Tibetan Plateau focused on temperature (Bräuning and Mantwill 2004; Gou et al. 2007; Fan et al. 2010; Duan and Zhang 2014; He et al. 2014; Wang et al. 2014; Liang et al. 2016; Li and Li 2017; Li et al. 2018, 2020, 2021) and precipitation (Sheppard et al. 2004; Shao et al. 2005; Liu et al. 2006b; Yang et al. 2014).

The eastern areas of the Tibetan Plateau, with average altitudes above 3000 m a.s.l., is the transition zone from the Plateau to the Sichuan Basin. To some extent, abundant sunshine makes up for the heat loss at high altitudes so that trees grow to a higher elevations, an optimal condition for maximizing climate signals in tree-rings. Therefore, the eastern plateau area is an ideal location for tree-ring studies of long-term climate change (Li et al. 2010). In past decades, climate reconstructions have been carried out in the eastern Tibetan Plateau, especially using average temperatures (Wu et al. 2005; Duan et al. 2010; Li et al. 2010, 2014; Yu et al. 2012b; Xiao et al. 2013a, 2015a, b; Deng et al. 2014), maximum temperatures (Qin et al. 2008; Xiao et al. 2013b; Zhu et al. 2016) and minimum temperatures (Shao and Fan 1999; Song et al. 2007; Yu et al. 2012a). These studies haven shown that tree growth in the eastern Tibetan Plateau is largely limited by temperature. Nevertheless, these studies have only revealed past climate changes in parts of the plateau and were largely based on tree species such as *Picea asperata* Mast., *Abies georgei*, or *Abies fabri* (Mast.) Craib. Other tree species in the mixed forests can be further used for dendrochologoical studies in the region.

The aims of this study were to: (1) develop tree-ring width chronologies of the Sichuan juniper (*Sabina saltuaria* Rehd. & Wilson) and Farges' fir (*Abies faxoniana* Rehd. & Wilson) on the eastern Tibetan Plateau, and compare their responses to climate factors; (2) reconstruct past climate changes based on climate-tree growth relationships; and (3) identify possible driving mechanisms of climate change in the region.

Materials and methods

Study site

The study site is located in the Liangtai valley (31.39° N, 102.89° E, at 3555 m a.s.l.) in the central Qionglai Mountains on the eastern Plateau (Fig. 1). This region has cool summers and cold winters, with annual mean temperatures of 6.9–11 °C and annual total precipitation of 650–1000 mm. There are extensive mixed forests in the valley, and the dominant vegetation includes *Sibiraea laevigata*, *Rhododendron*

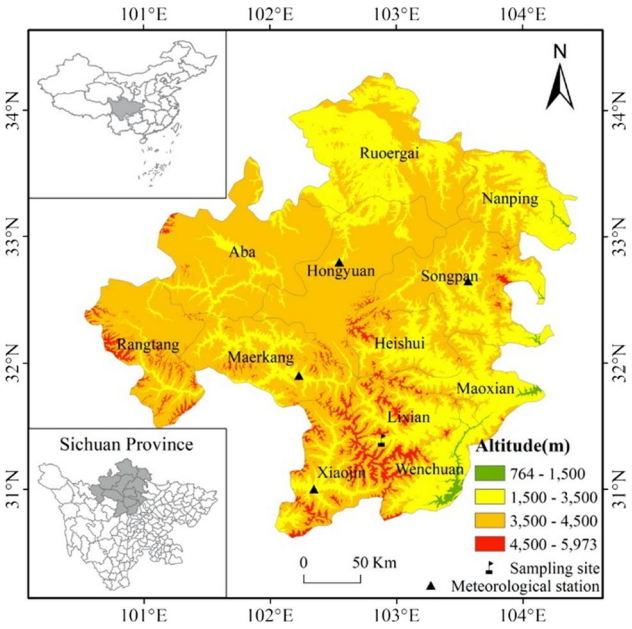

Fig. 1 Location of the study site (flag) and nearby meteorological stations (triangles)

simsii, *Larix mastersiana*, *Salix cupularis* and *Lonicera japonica* Thunb., similar to nearby Bipeng valley (Lin et al 2019). Dark brown soil occurs on slope deposits (Wu et al. 2010).

Tree-ring data

Tree core samples from *S. saltuaria* and *A. faxoniana* were collected in June 2017. One or two cores were taken from canopy-dominant, healthy trees in different directions at breast height (1.3 m above ground) using 5.15 mm increment borers. Twenty-two and 37 cores from 11 and 19 trees were obtained from *S. saltuaria* and *A. faxoniana,* respectively.

Standard dendrochronological methods of Cook and Kairiukstis (1990) were followed to prepare the core samples. The samples were air-dried, mounted on wooden slots, sanded with different grades of sandpaper (150–800 meshs) until cells and individual tracheids within annual rings were clearly discernible under the microscope. After visually cross-dating, ring widths were measured using the Velmex measuring system with a precision of 0.001 m (Bloomfield, NY, USA). The quality of cross-dating and measurement accuracy were statistically checked by the COFECHA program (Holmes 1983). Cores with low inter-series correlation were removed to prevent adding noise in chronology development. Finally, 19 and 34 cores from 10 and 19 trees were retained from *S. saltuaria* and *A. faxoniana*, respectively (Table 1).

Individual ring-width series were detrended to reduce the loss of low-frequency signals from tree age and stand

Table 1 Statistical characteristics of tree-ring chronologies of the two species

Statistics	*A. faxoniana*	*S. saltuaria*
Samples size (core/tree)	34/19	19-Oct
Samples mean sensitivity	0.19	0.251
Chronological mean sensitivity	0.13	0.158
Time span (years)	1754–2016	1418–2016
Time span with SSS > 0.85 (year)	1845–2016	1605–2016
Common period	1910–2016	1910–2012
Mean inter-series correlation (R1)	0.241	0.254
Mean correlation within a tree (R2)	0.592	0.568
Mean correlation between trees (R3)	0.229	0.236
Signal-to-noise ratio (SNR)	8.871	4.777
Expressed population signal (EPS)	0.899	0.827

dynamics by fitting a conservative negative exponential curve or linear curve with negative or zero slope using the ARSTAN program (Cook and Holmes 1986). The robust biweight mean was used to build the chronology from the standardized tree-ring series (Cook and Kairiukstis 1990). The subsample signal strength (SSS) of 0.85 was employed to identify the reliable period of the chronologies (Wigley et al. 1984). The statistical characteristics of the tree-ring width standard chronologies are shown in Table 1 and the chronologies in Fig. 2.

Climate data

Climate data were obtained from four meteorological stations (Xiaojin, Maerkang, Hongyuan and Songpan, Table 2) from the China Meteorological Data Sharing Service System (https://data.cma.cn/). Monthly mean (Tmean), maximum (Tmax) and minimum (Tmin) temperatures and monthly total precipitation (P) were used. To minimize spatial heterogeneity, records from the four meteorological stations were averaged to build regional monthly temperature and precipitation records. Based on climate data from 1961 to 2016, the regional annual Tmean was approximately 7.2 °C, with the monthly Tmean above 0 °C from February to November. Annual total precipitation was approximately 720 mm largely concentrated in May to September (Fig. 3).

Statistical analysis

The relationship of the two chronologies of the two species with regional climatic factors were analyzed using DendroClim2002 (Biondi and Waikul 2004), with 21 months of window from the previous March to the current November. Based on the climate-growth relationship, a simple linear

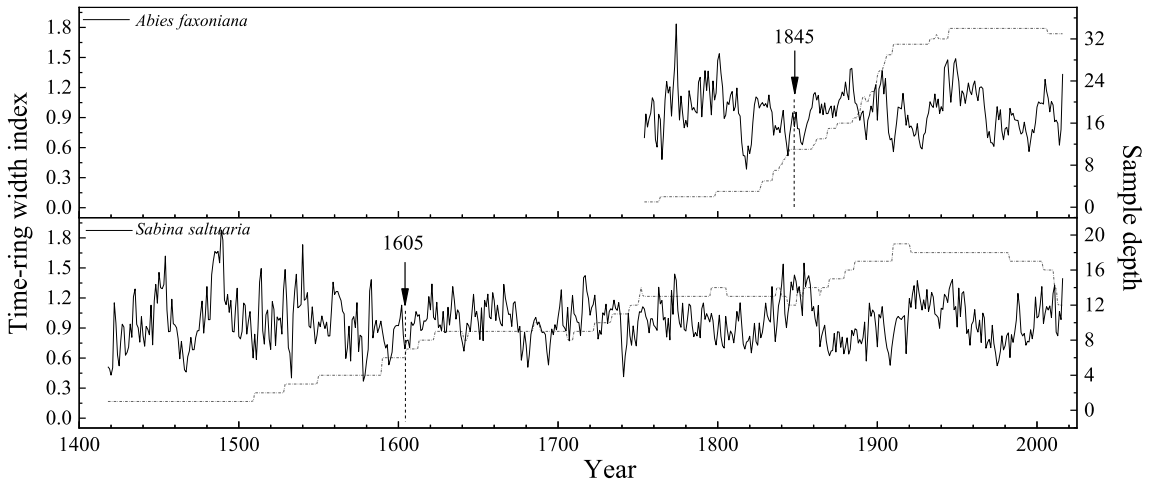

Fig. 2 Tree-ring width chronology (solid line) and sample depth (dotted line) from *A. faxoniana* and *S. saltuaria.* Vertical dashed line denotes SSS > 0.85

Table 2 Information of four weather stations near the sampling site

Weather stations	Latitude (N)	Longitude (E)	Elevation (m)	Period
Xiaojin	31	102.21	2438	1952–2016
Maerkang	31.54	102.14	2664.4	1954–2016
Hongyuan	32.48	102.33	3491.6	1961–2016
Songpan	32.4	103.36	2881.3	1951–2016

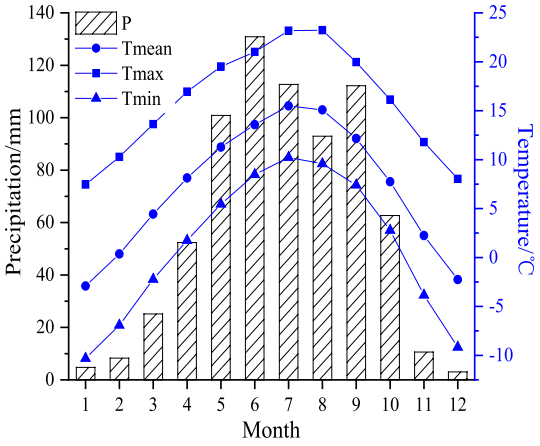

Fig. 3 Monthly mean (Tmean), maximum (Tmax), minimum (Tmin) temperatures and monthly total precipitation (P) from regional meteorological data (1961–2016). Months of 1–12 indicate January to December

regression model (Cook and Kairiukstis 1990) was developed for reconstruction.

The traditional split sample calibration-verification method tested the reliability of the reconstruction model (Cook and Kairiukstis 1990). Statistical parameters, including Pearson's correlation coefficient (r), the coefficient of determination (R^2), the sign test (ST), the reduction of error (RE), the coefficient of efficiency (CE) and the Durbin–Watson (D/W) test, were used to evaluate the reconstruction model (Fritts 1976; Cook and Kairiukstis 1990). Positive values of RE and CE are considered to be good indicators of an appropriate model (Cook et al. 1999).

An 11-year moving average method was applied to explore multidecadal changes of the reconstruction. Spectral analyses were performed using the Multi-Taper Method (MTM; Mann and Lees 1996) and wavelet analysis (Torrence and Compo 1998) to explore the periodic variations of the reconstructed series. Spatial correlations between the observed and reconstructed series and 0.5° × 0.5° gridded CRU TS4.03 temperature data (Harris et al. 2014) were calculated using the KNMI climate explorer (http://climexp.knmi.nl/) to understand regional representativeness. In order to investigate the impacts of global sea surface temperatures on climate varaiblity in the study area, the global extended reconstructed sea surface temperature version 4 dataset (ERSST v4) was adopted for spatial correlations (Huang et al. 2015).

Results

Climate-growth relationships of the two species

Growth of *A. faxoniana* and *S. saltuaria* was positively correlated with most regional temperature parameters. There were significant positive correlations between annual rings of *A. faxoniana* and regional Tmean in the previous April and October and the current October (Fig. 4a). The growth of *A. faxoniana* was also positive with regional Tmax in the previous September and October and the current October

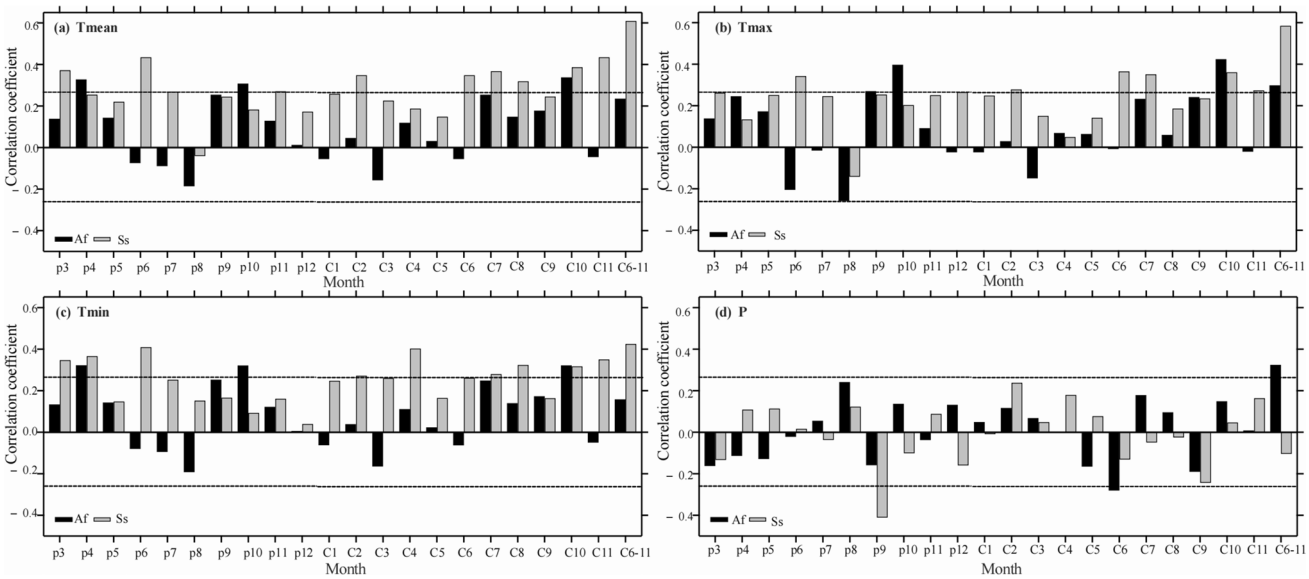

Fig. 4 Correlations between climate factors (Tmean, Tmax, Tmin, P) and chronologies of *A. faxoniana* (Af) and *S. saltuaria* (Ss) during 1961–2016. Months of p3–p12 indicate previous March to previous December; Months of C1–C11 indicate current January to current November; C6–11 (current June to November) represents the target season for reconstruction; horizoental dashed lines denote 95% confidence level

(Fig. 4b). Significant positive correlations were found with regional Tmin in the previous April and October and the current October (Fig. 4c).

Growth of *S. saltuaria* had similar relationships with temperatures; it was significantly positive with regional Tmean in the previous March, June, and November, and the current February, June–August, and October–November (Fig. 4a). Growth was positively related to the regional Tmax in the previous June and December, and the current February, June–July, and October–November (Fig. 4b) as well as regional Tmin in the previous March–April, June, and the current February, April, July–August, and October–November (Fig. 4c). At the same time, growth of both species was weakly related with precipitation despite negative correlations with *S. saltuaria* in the previous September and with *A. faxoniana* in the current June (Fig. 4d).

Generally seasonal climate was more likely to influence growth than monthly climatic variables. Therefore, correlations between different combinations of regional monthly climatic factors and chronologies of *A. faxoniana* and *S. saltuaria* were further explored to determine if there was a limiting climatic factor on growth. The results show that the chronology of *S. saltuaria* had the highest correlation with regional Tmean in the current June-November period (T_{6-11}, $r=0.610$, $p<0.001$), indicating that it was the main limiting factor on *S. saltuaria* growth.

Regional T_{6-11} reconstruction

With the limiting factor of regional T_{6-11} on *S. saltuaria* growth, a simple linear regression model between the *S. saltuaria* chronology and regional T_{6-11} was developed to reconstruct past temperature changes. The model is:

$$T_{6-11} = 1.587 \times W_t + 9.606$$
$$\left(N = 56, r = 0.610, R^2 = 37.3\%, R^2adj = 36.1\%, F = 32.084, p < 0.0001, \mathrm{D/W} = 1.647\right)$$

where T_{6-11} is the regional mean temperature from June to November, W_t is the ring-width index at year t. The reconstruction model accounted for 37.3% (36.1% after adjusting for the degree of freedom) of the regional Tmean variance from 1961 to 2016. The D/W test value (Durbin and Watson 1950) was 1.647 (Table 3), which indicated that there was no significant autocorrelation or linear trend in the residuals. The split-sample calibration and verification method tested the stability and reliability of the reconstruction model (Table 3). The generally positive RE and CE values for verification indicated that the regression model was reliable for reconstruction (Cook et al. 1999), although the CE value was slightly negative during 1961–1988. Almost all of these statistical parameters showed that the reconstruction model was stable and reliable. There was good consistency between the reconstructed and the observed series during 1961–2016 (Fig. 5a). Therefore, regional T_{6-11} since 1605 AD was reconstructed for the study region using the above regression model (Fig. 5b).

Regional temperature variations over the past 412 years

Based on the above regression model, regional T_{6-11} from 1605 to 2016 was reconstructed. Temperatures ranged from 10.3–12.1 °C with its mean of 11.1 °C (Fig. 5b). Based on mean ± σ, the extremely high temperature was defined as exceeding 11.5 °C and extremely low temperature below 10.8 °C. Therefore, the extremely high and low temperature years accounted for 15% (63 years) and 17% (71 years) of the past 412 years, respectively. The top five warmest years were 1854, 1841, 1773, 1848, and 1717, and the five coldest years were 1741, 1681, 1975, 1908 and 1694, respectively. Based on the 11-year moving average of the reconstructed series, there were six major warm periods (1612–1673, 1702–1737, 1754–1780, 1832–1863, 1916–1959, 2000–2016) and five major cold periods (1674–1701, 1738–1753, 1781–1831, 1864–1915, 1960–1999) in the past 412 years.

Periodic variation of the reconstructed series

Multi-Taper Method (MTM) spectral analysis indicated several important periodicities in the reconstructed temperature series (Fig. 6). Significant periodic oscillations of

Table 3 Calibration and verification statistics for regional T_{6-11} reconstruction

	r	R^2	CE	RE	ST	D/W
Calibration (1961–1988)	0.338*	0.114	–	–	19+ /9–	2.194
Verification (1961–1988)	0.338*	0.114	–0.039	0.609	19+ /9–	2.194
Calibration (1989–2016)	0.597**	0.357	–	–	22+ /6–**	1.531
Verification (1989–2016)	0.597**	0.357	0.263	0.725	22+ /6–**	1.531
Full calibration (1961–2016)	0.610**	0.373	–	–	41+/15–**	1.647

*Significance at the 95% confidence level, **Significance at the 99% confidence level

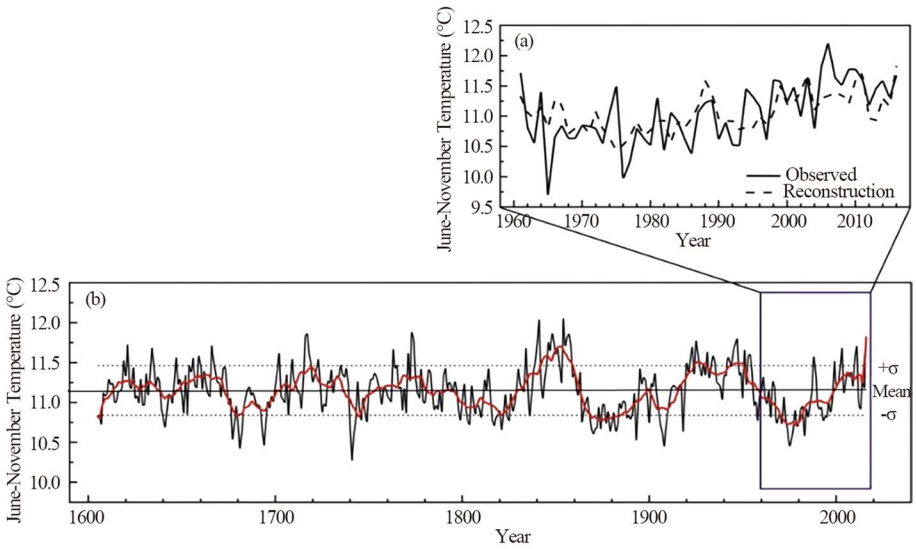

Fig. 5 **a** Comparison of observed (solid line) and reconstructed (dashed line) regional $T_{6\text{-}11}$ during 1961–2016; **b** the reconstructed (thin line) regional $T_{6\text{–}11}$ and its 11-year moving average (thick line) during 1605–2016

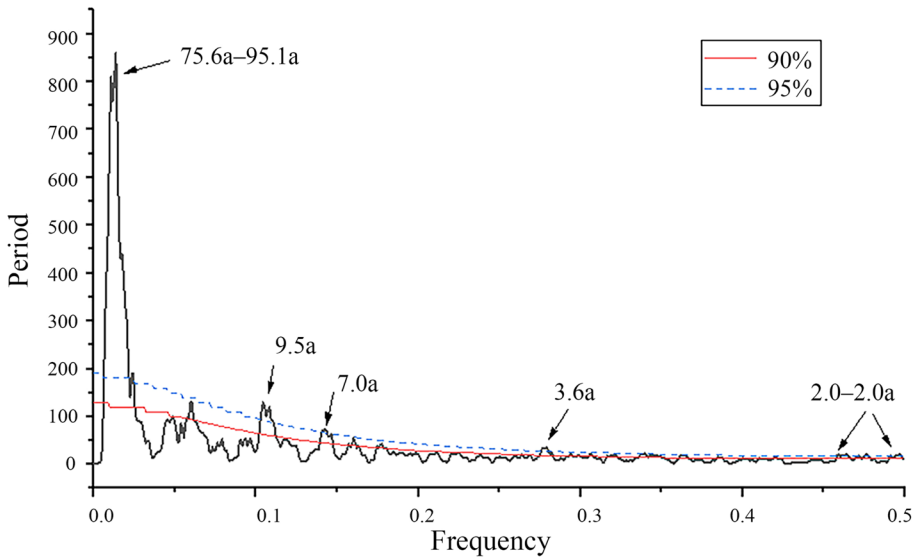

Fig. 6 MTM spectral analysis of the reconstructed $T_{6\text{–}11}$ 1605–2016. Solid and dashed lines denotes 90% and 95% confidence levels respectively

interannual (2.0–2.2a, 3.6a, 7.0a, 9.5a) and multi-decadal (75.6–95.1a) timescales at 95% significance were found over 1605–2016. Wavelet analysis showed that the interannual cycles were the main periods of temperature change over the full reconstruction period, while the multi-decadal cycle was most pronounced over 1800–2000 (Fig. 7).

Discussion

Climate-growth response of the two species

Based on correlations between tree-ring chronologies and regional climatic factors, that temperature in most months was positively correlated with *S. saltuaria* and *A. faxoniana* growth (Fig. 4). The study area is influenced by the monsoon climate with high rainfalls and cool summers due to the terrain. Rainy weather with increased cloud cover reduces solar radiation and also lowers temperatures. Therefore, temperatures in the growing season, especially during June–November, had considerable influence on regional tree growth (Yu et al. 2012b; Zhu et al. 2016). Increasing temperatures in the growing season enhances photosynthesis and stimulates cell division, is conducive to radial growth when a minimum temperature threshold is reached (Shao and Fan 1999; Qin et al. 2008; Xiao et al. 2015a; Li et al. 2017). Therefore, temperature was the critical factor controlling tree growth in the eastern Tibetan Plateau when precipitation was abundant in the growing season.

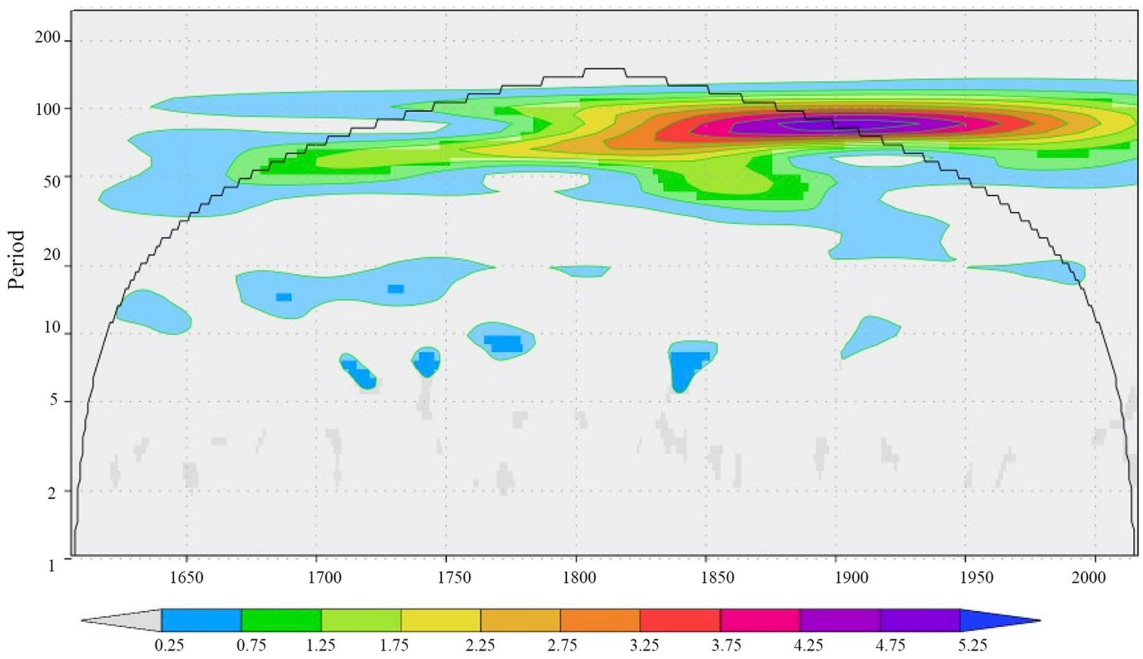

Fig. 7 Wavelet analysis of the reconstructed T6–11 during 1605–2016

Spatial representativeness of the reconstruction

To explore the regional representativeness of the reconstructed $T_{6–11}$, a spatial correlation analysis was performed using the actual and reconstructed $T_{6–11}$ with 0.5° × 0.5° gridded CRU TS4.03 temperature from 1961 to 2016 (Fig. 8). The results indicate that spatial correlation patterns are consistent between the actual and reconstructed $T_{6–11}$ series over the eastern Tibetan Plateau, albeit the correlations are slightly weaker for the reconstruction. Both series have significant positive correlations, suggesting that the reconstructed $T_{6–11}$ can represent regional temperature changes over the past four centuries.

To validate regional representativeness of the reconstructed $T_{6–11}$, annual temperatures from the previous September to the current August ($T_{9–8}$) in Songpan (Li et al. 2014) and the July temperature (T_7) reconstruction in Maerkang (Yu et al. 2012b) were compared (Fig. 9a, b, c). Three reconstructions exhibit similar temperature variations: the warm periods of 1700s–1730s, 1840s–1850s, 1940s–1960s, 2000s–2010s, and the cold periods of 1670s–1690s, 1810s–1830s, 1970s–1990s. Similar results have also been

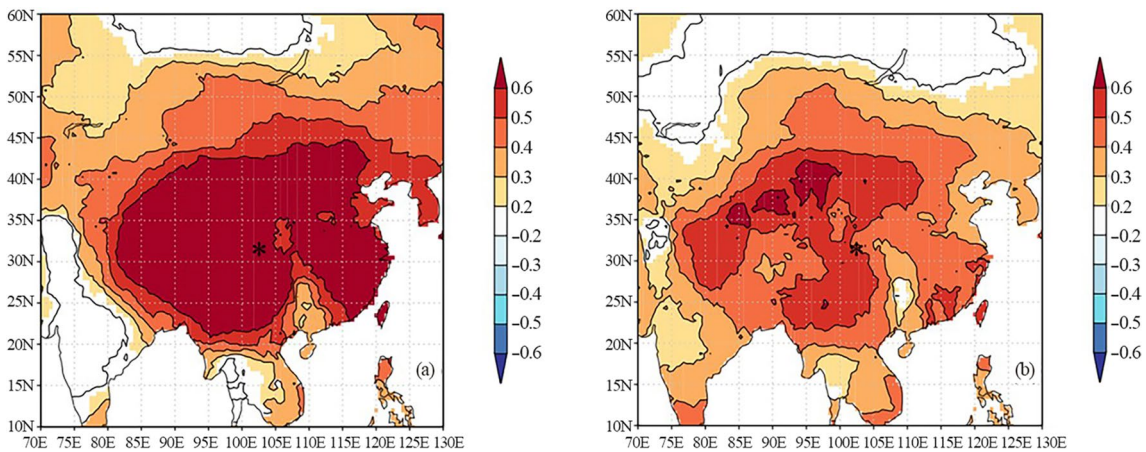

Fig. 8 Spatial correlations of the **a** actual and **b** reconstructed $T_{6–11}$ with CRU TS4.03 temperatures during 1961–2016. The star denotes the sampling site

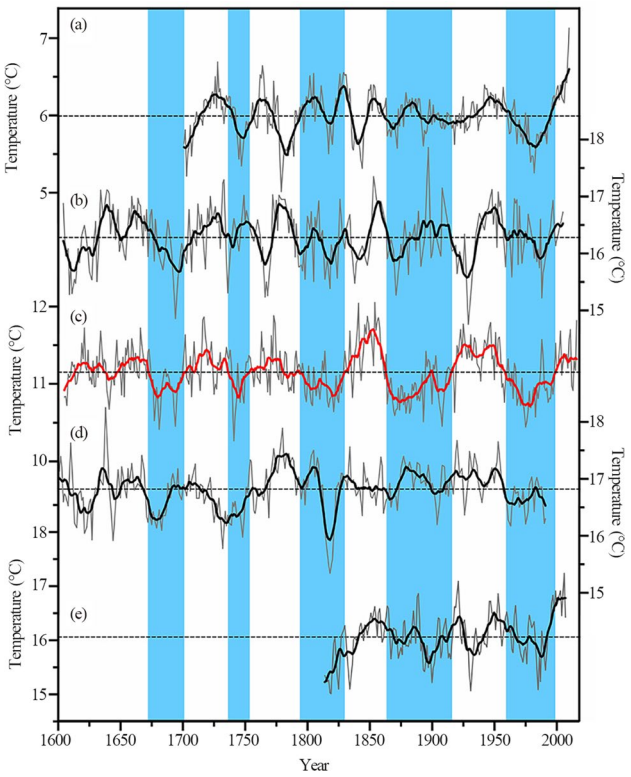

Fig. 9 Comparison of **a** $T_{9–8}$ in Songpan (Li et al. 2014), **b** T_7 in Mearkang (Yu et al. 012b), **c** $T_{6–11}$ in Liangtai valley (this study), **d** T_{2-6} in Kathmandu (Cook et al. 2003), **e** $T_{5–9}$ in Arxan, Inner Mongolia (Liu et al. 2012). Bold lines denote 11-year moving average in each panel, blue shading denotes major cold periods in the T_{6-11} reconstruction

noted in other regions of the eastern Tibetan Plateau (Shao and Fan 1999; Yu et al. 2012a; Xiao et al. 2013a, 2015a).

To verify the spatial representativeness of the reconstructed $T_{6–11}$ at a larger scale, it was further compared with the February–June ($T_{2–6}$) reconstruction in the Himalayas (Cook et al. 2003), and the May–September ($T_{5–9}$) reconstruction in Arxan, Inner Mongolia (Liu et al. 2012). The three reconstruction series were consistent of the low temperature periods in the 1810s–1830s and 1970s–1990s, and in the warm period in the 1940s–1960s, suggesting a synchronized temperature change at a large scale (Fig. 9c, d, e).

The tree-ring based temperature reconstructions are also consistent with the advance and retreat of the Hailuogou Glacier (Li et al. 2008, 2009; Liu et al. 2006a; Xiao et al. 2015a) on the eastern Tibetan Plateau. The glacier retreated during the 1930s–1960s, corresponding to a warm period in the T_{6-11} reconstruction. During the 1970s–1980s, the glacier was relatively stable or retreated slowly, reflecting a continuous period of low temperatures. Since the mid-1980s, the glacier has been in a stage of rapid retreat and the reconstructed $T_{6–11}$ showed temperature increases due to global warming (IPCC 2013).

Possible driving mechanisms

The results of MTM and wavelet analyses revealed significant cycles in the reconstructed temperatures (Figs. 6, 7). The 2–7a and 9.5a periods were consistent with the periodic changes of the El Nino–Southern Oscillation (Song et al. 2007; Li et al. 2010; Yu et al. 2012b; Xiao et al. 2013b; Zhu et al. 2016) and solar activity (Xiao et al. 2013b, 2015b). The 75.6–95.1a cycle may be related to the Atlantic Multidecadal Oscillation (Zhu et al. 2016).

Oceans regulate atmospheric circulation and world climate variability (Cai and Liu 2017), and are strongly connected with regional climates. Spatial correlations of the observed and reconstructed $T_{6–11}$ with global sea surface temperature during 1961–2016 showed a similar spatial correlation, with positive correlations in the western Pacific and North Atlantic oceans (Fig. 10). The relationship of our temperature reconstructions were further vertified with the Atlantic Multidecadal Oscillation by calculating their

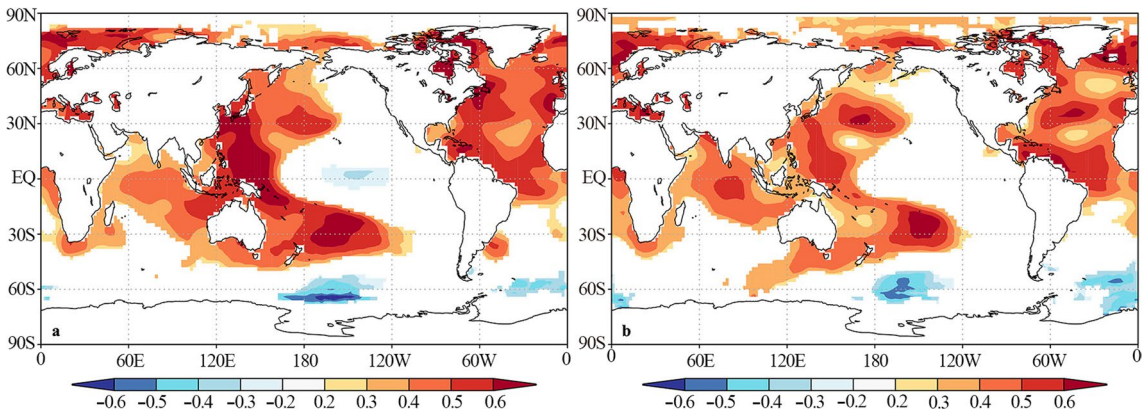

Fig. 10 Spatial correlations of the **a** observed and **b** reconstructed $T_{6–11}$ with global ERSST v4 SSTs in $T_{6–11}$ over the period 1961–2016

correlations over the period 1880–2016. The results indicate that our temperature reconstructions had a positive correlation ($r = 0.385$, $p < 0.01$) during the period. This is consistent with studies showing the influence of the Atlantic Multidecadal Oscillation on the eastern Tibetan Plateau (Wang et al. 2014; Liang et al. 2016; Li and Li 2017; Li et al. 2021). The warm-phase of the Atlantic Multidecadel Oscillation in summer can trigger positive geopotential height anomalies in the subtropical western Pacific and strong subtropical anticyclones, which further strengthen the East Asian summer monsoon (Lu et al. 2006; Wang et al. 2009). In addition, the warm-phase in winter can cause strong midlatitude westerly winds and extend the North Atlantic low surface air pressure to the Eurasian continent, leading to a weakened East Asian winter monsoon (Dong et al. 2006; Li and Bates 2007; Wang et al. 2009; Ding et al. 2014). The warm-phase may also heat the Asian continent troposphere via the mid- and high-latitudes Rossby wave propagation (He et al. 2014; Wang et al. 2014). Therefore, it may have a crucial influence on temperature variability in the region.

Conclusions

In this study, tree-ring width chronologies of *S. saltuaria* and *A. faxoniana* from the mixed forests on the eastern Tibetan Plateau were developed. The results indicate that the radial growth of both species was strongly influenced by temperature. The strongest relationship was found between annual rings of *S. squamata* and regional mean temperatures from June to November ($T_{6–11}$). Based on this relationship, a regional $T_{6\text{-}11}$ was reconstructed for the period 1605–2016. Spatial correlation analysis and comparison with other temperature reconstructions revealed that our reconstruction represented large-scale temperature changes on the plateau and showed a strong warming trend since the 1980s, suggesting that tree growth tracks well the warming signals in the region. Moreover, our records exihibit a linkage with the Atlantic Multidecadel Oscillation, providing new evidence on its influence on climate change over the eastern Tibetan Plateau.

References

Biondi F, Waikul K (2004) Dendroclim 2002: A C ++ program for statistical calibration of climate signals in tree-ring chronologies. Comput Geosci 30:303–311

Bräuning A, Mantwill B (2004) Summer temperature and summer monsoon history on the Tibetan Plateau during the last 400 years recorded by tree rings. Geophys Res Lett 31:L24205

Cai QF, Liu Y (2017) Two centuries temperature variations over subtropical southeast China inferred from *Pinus taiwanensis* Hayata tree-ring width. Clim Dynam 48:1813–1825

Cook ER, Holmes RL (1986) Users manual for ARETAN: laboratory of tree-ring research. University of Arizona, Tucson, pp 50–60

Cook ER, Kairiukstis LA (1990) Methods of dendrochronology, applications in the environmental sciences. Kluwer, Dordrecht

Cook ER, Meko DM, Stahle DW, Cleaveland MK (1999) Drought reconstructions for the continental United States. J Clim 12:1145–1162

Cook ER, Krusic PJ, Jones PD (2003) Dendroclimatic signals in long tree-ring chronologies from the Himalayas of Nepal. Int J Climatol 23(7):707–732

Deng Y, Gou XH, Gao LL, Yang T, Yang MX (2014) Early summer temperature variations over the past 563 yr inferred from tree rings in the Shaluli Mountains, southeastern Tibet Plateau. Quat Res 81(3):513–519

Ding YH, Liu YJ, Liang SJ, Ma XQ, Zhang YX, Si D, Liang P, Song YF, Zhang J (2014) Interdecadal variability of the East Asian winter monsoon and its possible links to global climate change. J Meteor Res 28:693–713

Dong BW, Sutton RT, Scaife AA (2006) Multidecadal modulation of El Nino-Southern Oscillation (ENSO) variance by Atlantic Ocean sea surface temperatures. Geophys Res Lett 33:L08705

Duan JP, Zhang QB (2014) A 449 year warm season temperature reconstruction in the southeastern Tibetan Plateau and its relation to solar activity. J Geophys Res: Atmos 119:11578–11592

Duan JP, Wang LL, Li L, Chen KL (2010) Temperature variability since AD 1837 inferred from tree-ring maximum density of Abies fabric in Gongga Mountains China. Chin Sci Bull 55(11):1036–1042

Durbin J, Watson GS (1950) Testing for serial correlation in least squares regression. I Biometrika 37:409–428

Fan ZX, Brauning A, Tian QH, Yang B, Cao KF (2010) Tree ring recorded May–August temperature variations since A.D. 1585 in the Gaoligong Mountains. Southeastern 296:94–102

Fritts HC (1976) Tree rings and climate. Academic Press, New York

Gou XH, Chen FH, Jacoby G, Cook E, Yang MX, Peng JF, Zhang Y (2007) Rapid tree growth with respect to the last 400 years in response to climate warming, northeastern Tibetan Plateau. Int J Climatol 27:1497–1503

Gou XH, Deng Y, Chen FH, Yang MX, Fang KY, Gao LL, Yang T, Zhang F (2010) Tree ring based streamflow reconstruction for the Upper Yellow River over the past 1234 years. Chin Sci Bull 55(36):4179–4186

Harris I, JonesD OTJ, Lister DH (2014) Updated high-resolution grids of monthly climatic observations—the CRU TS3. 10 Dataset. Int J Climatol 34:623–642

He MH, Yang B, Datsenko NM (2014) A six hundred-year annual minimum temperature history for the central Tibetan Plateau derived from tree-ring width series. Clim Dynam 43:641–655

Holmes RL (1983) Computer-assisted quality control in tree-ring dating and measurement. Tree-Ring Bull 43:69–75

Huang BY, Banzon V, Freeman E, Lawrimore J, Liu W, Peterson TC, Smith TM, Thorne PW, Woodruff SD, Zhang HM (2015) Extended reconstructed sea surface temperature version 4

(ERSST.v4). Part I: upgrades and Intercomparisons. J Climate 28:911–930

IPCC (2013) Climate change 2013: the physical science basis. Contribution of working group I to the fifth assessment report of the intergovernmental panel on climate change. Cambridge University Press, Cambridge and New York, NY

Li SL, Bates GT (2007) Influence of the Atlantic multidecadal oscillation on the winter climate of East China. Adv Atmos Sci 24:126–135

Li T, Li JB (2017) A 564-year annual minimum temperature reconstruction for the east central Tibetan Plateau from tree rings. Global Planet Change 157:165–173

Li ZX, He YQ, Jia WX, Pang HX, Yuan LL, Ning BY, Liu Q, He XZ, Song B, Zhang NN (2008) Response of "Glaciers-Runoff" system in a typical temperature-glacier, Hailuogou Glacier in Gongga Mountain of China to global change. Scientia Geographica Sinica 28(2):229–234 (**in Chinese**)

Li ZX, He YQ, Jia WX, Pang HX, He XZ, Wang SJ, Zhang NN, Zhang WJ, Liu Q, Xin HJ (2009) Changes in Hailuogou glacier during the recent 100 years under global warming. J Glaciol Geocryol 31(1):75–81 (**in Chinese**)

Li ZS, Liu GH, Zhang QB, Hu CJ, Luo SZ, Liu XL, He F (2010) Tree ring reconstruction of summer temperature variations over the past 159 years in Wolong National Natural Reserve, western Sichuan. China Chin J Plant Ecol 34(6):628–641 (**in Chinese**)

Li JJ, Shao XM, Li YY, Qin NS (2014) Annual temperature recorded in tree-ring from Songpan region. Chin Sci Bull 59(15):1446–1458

Li X, Liang E, Gričar J, Rossi S, Čufar K, Ellison AM (2017) Critical minimum temperature limits xylogenesis and maintains treelines on the southeastern Tibetan Plateau. Sci Bull 62(11):804–812

Li MY, Duan JP, Wang LL, Zhu HF (2018) Late summer temperature reconstruction based on tree-ring density for Sygera Mountain, southeastern Tibetan Plateau. Global Planet Change 163:10–17

Li JX, Li JB, Li T, Au TF (2020) Tree growth divergence from winter temperature in the Gongga Mountains, southeastern Tibetan Plateau. Asian Geogr 37(1):1–15

Li JX, Li JB, Li T, Au TF (2021) 351-year tree ring reconstruction of the Gongga Mountains winter minimum temperature and its relationship with the Atlantic Multidecadal Oscillation. Clim Chang 165:1–19

Liang HX, Lyu LX, Wahab M (2016) A 382-year reconstruction of August mean minimum temperature from tree-ring maximum latewood density on the southeastern Tibetan Plateau, China. Dendrochronologia 37:1–8

Lin PJ, Li CY, Lu CT, Wang G, Yang L, Liu QC (2019) Analysis of red color-leafed forest landscape stability in Bipeng Valley Scenic Spots. J Sichuan Forest Sci Technol 40(4):7–11 (**in Chinese**)

Liu XD, Chen BD (2000) Climatic warming in the Tibetan Plateau during recent decades. Int J Climatol 20:1729–1742

Liu XD, Zhang MF (1998) Contemporary climatic change over the Qinghai- Xizang Plateau and its response to the Green-House effect. Chin Geogr Sci 8(4):289–298

Liu SY, Ding YJ, Li J, Shangguan DH, Zhang Y (2006a) Glaciers in response to recent climate warming in Western China. Quaternary Sci 26(5):762–771 (**in Chinese**)

Liu Y, An ZS, Ma HZ, Cai QF, Liu ZY, Kutzbach JK, Shi JF, Song HM, Sun JY, Yi L, Li Q, Yang YK, Wang L (2006) Precipitation variations recorded by tree rings in Dulan area of Qinghai Province since 850 A.D. and their relationship with temperature in the Northern Hemisphere. Sci China Series D Earth Sci 36(5):461–471

Liu Y, An ZS, Linderholm HW, Chen DL, Song HM, Cai QF, Sun JY, Tian H (2009) Annual temperatures during the last 2485 years in the mid-eastern Tibetan Plateau inferred from tree rings. Sci China Series D Earth Sci 52(3):348–359

Liu Y, Xiang N, Song HM (2012) Tree-ring temperature records in Arxan, Inner Mongolia for the past 187 years. J Earth Environ 3(3):862–867 (**in Chinese**)

Lu RY, Dong BW, Ding H (2006) Impact of the Atlantic multidecadal oscillation on the Asian summer monsoon. Geophys Res Lett 33:L24701

Mann ME, Lees JM (1996) Robust estimation of background noise and signal detection in climatic time series. Clim Chang 33:409–445

Peng JF, Liu YZ, Wang T (2014) A tree-ring record of 1920's—1940's droughts and mechanism analyses in Henan Province. Acta Ecol Sin 34(13):3509–3518 (**in Chinese**)

Qin NS, Shi XH, Shao XM, Wang QC (2008) Average maximum temperature change recorded by tree rings in West Sichuan Plateau. Plateau and Mountain Meteorology Research 28(4):18–24 (**in Chinese**)

Schweingruber FH (1996) Tree rings and environment dendroecology. Paul Haupt Verlag, Bern

Shao XM (1997) Advancements in dendrochronology. Quaternary Sci 17(3):265–271 (**in Chinese**)

Shao XM, Fan JM (1999) Past climate on west Sichuan Plateau as reconstructed from ring-widths of dragon spruce. Quater Sci 1:81–89 (**in Chinese**)

Shao XM, Huang L, Liu HB, Liang EY, Fang XQ, Wang LL (2005) Reconstruction of precipitation variation from tree rings in recent 1000 years in Delingha, Qinghai. Sci China Ser D Earth Sci 48(7):939–949

Sheppard PR, Tarasov PE, Graumlich LJ, Heussner KU, Wagner M, Osterle H, Thompson LG (2004) Annual precipitation since 515 BC reconstructed from living and fossil juniper growth of northeastern Qinghai Province, China. Clim Dynam 23:869–881

Song HM, Liu Y, Ni WM, Cai QF, Sun JY, Ge WB, Xiao WY (2007) Winter mean lowest temperature derived from tree ring width in Jiuzhaigou region, China since 1750 AD. Quaternary Sci 27(4):486–491

Torrence C, Compo GP (1998) A practical guide to wavelet analysis. Bull Am Meteorol Soc 79:61–78

Wang YM, Li SL, Luo DH (2009) Seasonal response of Asian monsoonal climate to the Atlantic Multidecadal Oscillation. J Geophys Res Atmos 114:D02112

Wang JL, Yang B, Qin C, Kang SY, He MH, Wang ZY (2014) Tree-ring inferred annual mean temperature variations on the southeastern Tibetan Plateau during the last millennium and their relationships with the Atlantic Multidecadal Oscillation. Clim Dynam 43:627–640

Wigley TML, Briffa KR, Jones PD (1984) On the average value of correlated time series, with applications in dendroclimatology and hydrometeorology. J Appl Meteorol Climatol 23:201–213

Wu P, Wang LL, Shao XM (2005) Reconstruction of summer temperature from maximum latewood density of *Pinus densata* in West Sichuan. Acta Geogr Sin 60(6):998–1006 (**in Chinese**)

Wu FZ, Yang WQ, Zhang J, Deng R (2010) Fine root decomposition in two subalpine forests during the freeze-thaw season. Can J Forest Res 40:298–307

Xiao DM, Qin NS, Li JJ, Li YY (2013a) Variations of June air temperature derived from tree-ring records in 1713–2010 in Jinchuan, west Sichuan Plateau, China. Progressus Inquisitiones De Mutatione Climatis 9(4):252–257 (**in Chinese**)

Xiao DM, Qin NS, Li JJ, Li YY (2013b) Change of mean maximum temperature in July during 1506–2008 in Seda of west Sichuan Plateau according to reconstructed tree-ring series. J Desert Res 33(5):1536–1543 (**in Chinese**)

Xiao DM, Qin NS, Huang XM (2015a) A 325-year reconstruction of July–August mean temperature in the north of west Sichuan derived from tree-ring. Quaternary Sciences 35(5):1134–1144 (**in Chinese**)

Xiao DM, Qin NS, Li JJ, Li YY, Mu L (2015b) Change of mean temperature from July to September in Northeast of Western Sichuan Plateau based tree-ring. Plateau Meteorology 34(3):762–770 (**in Chinese**)

Yang B (2012) Spatial and temporal patterns of climate variations over the Tibetan Plateau during the period 1300–2010. Quaternary Sci 32(1):81–94 (**in Chinese**)

Yang B, Qin C, Wang JL, He MH, Melvin TM, Osborn TJ, Briffa KR (2014) A 3,500-year tree-ring record of annual precipitation on the northeastern Tibetan Plateau. Proc Natl Acad Sci USA 111:2903–2908

Yu SL, Yuan YJ, Wei WS, Shang HM, Zhang TW, Chen F, Zhang RB (2012a) Reconstruction of minimum temperature field in June–July during 1787–2005 in the West Sichuan Plateau. J Desert Res 32(4):1010–1016 (**in Chinese**)

Yu SL, Yuan YJ, Wei WS, Zhang TW, Shang HM, Chen F (2012b) Reconstructed mean temperature in Mearkang, West Sichuan in July and its detection of climatic period signal. Plateau Meteorol 31(1):193–200 (**in Chinese**)

Zhu LJ, Zhang YD, Li ZS, Guo BD, Wang XC (2016) A 368-year maximum temperature reconstruction based on tree-ring data in the northwestern Sichuan Plateau (NWSP), China. Clim past 12:1485–1498